Pure & Appl. Chem., Vol. 62, No. 9, pp. 1653–1660, 1990.
Printed in Great Britain.

Chemical properties of small silicon clusters

M. L. Mandich, W. D. Reents, Jr., and K. D. Kolenbrander

AT&T Bell Laboratories, Murray Hill, New Jersey 07974 USA

Abstract - The microscopic surfaces of small silicon clusters offer a model for studying chemistry at highly reactive silicon centers. Positively and negatively charged silicon clusters are prepared and reacted with a variety of reagents in the trapped ion cell of a Fourier transform mass spectrometer. Prototypical etching and deposition reactions are observed which are analogous to chemistry of activated silicon surfaces. These reactivities correlate with chemistry of two distinct types of dangling bonds in the clusters. Sequential reactions of bare silicon cluster and subsilane cations with silane also occur. All of these clustering sequences, however, encounter early bottlenecks which prevent infinite growth to form large particles. Studies of the individual steps of these clustering reactions yield extensive information about nucleation under subsaturated conditions. These findings indicate that reactions of silicon cluster and subsilane cations with silanes do not lead to the formation of hydrogenated silicon dust in silane plasmas.

INTRODUCTION

Silicon chemistry is the foundation of silicon device fabrication. Demands of VLSI and subminiaturization technology require precise control of silicon chemistry with a wide variety of reagents. Currently, the need for this chemistry is so great that processes are designed and used with little knowledge about the nature of the reactions. This leads to poor control over a wide range of processing conditions and often multiple steps must be used to prevent undesirable side reactions. Clearly, there is much to be gained by expanding our understanding of silicon chemistry.

Our approach is to study an analogous system: the microscopic surfaces on small silicon clusters. This offers the distinct advantage that the bimolecular reactivity of these clusters can be unambiguously studied with a wide variety of reagents. The geometric and electronic structures of these clusters are dramatically different from those of bulk silicon surfaces or stable silicon compounds such as silanes. Thus, the reactivity of these clusters may be most relevant to the reactivity of defects or rough silicon surfaces. Additionally, the reactive sites on these clusters may resemble the highly reactive silicon surfaces produced by the ion bombardment, photochemical activation, or heating often used in silicon device processing.

The departure of these clusters from bulk structures can be appreciated by comparing the energetics of alternative structures for Si_4 and Si_6 shown in Fig. 1. The structures on the left are obtained by "snipping" appropriate fragments from bulk silicon. The structures on the right are the lowest energy structures that have been calculated for these clusters using *ab initio* electronic structure theory (Refs. 1-4). The microcrystalline bulk fragments are much higher in energy than the ground state structures by 3.1 and 5.6 eV, respectively, for Si_4 and Si_6 (Ref. 2). Similar relative energies have also been found for the cationic silicon cluster ions (Ref. 5). The reason why the microcrystalline fragments are high energy species is because their silicon centers have a greater degree of unsaturation than those in the more compact ground state structures.

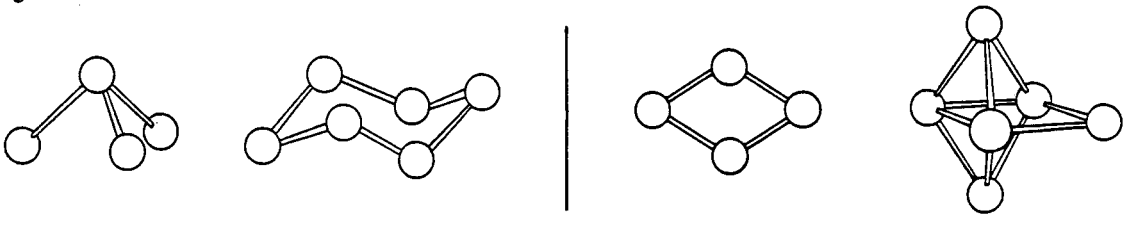

Fig. 1. Comparison of the microcrystalline fragment (left) and lowest energy (right) structures for Si_4 and Si_6 clusters. The structures on the right are also the lowest energy structures for the corresponding cationic clusters.

The silicon cluster structures in Fig. 1 are expected to be highly reactive. All of the silicon atoms are on the cluster "surface" which has a considerable number of dangling bonds available for chemical activity. Our studies of their reactions with various reagents have revealed a rich chemistry which, in many cases, is remarkably similar to chemistry of bulk silicon surfaces. This chemistry occurs readily at room temperature in the gas phase. For example, silicon cluster ions are "etched" by reagents such as XeF_2 and NO_2 in reactions which result in loss of silicon atoms from the clusters

(Refs. 6-8). Alternatively, organic and silane reagents react with positively charged clusters in processes which "deposit" moieties onto the cluster (Refs. 8-11). Different types of dangling bonds on the cluster appear to be involved in this prototypical etching versus deposition type reactivity.

The reactions of silicon clusters with SiD_4 have been particularly valuable systems for studying the microscopic effects of cluster structure on reactivity (Refs. 10-16). In these reactions, growth of larger silicon clusters occurs by addition of SiD_2 accompanied by loss of D_2. Many clusters undergo these reactions sequentially to form larger and larger species. Nonetheless, all silicon clusters encounter chemical constraints preventing unlimited growth. We have examined the mechanisms of these reactions using experimental results in concert with *ab initio* electronic structure calculations of the energetics and structures of various species. Our findings reveal new mechanisms for reactivity at silicon centers and have implications for the nucleation of detrimental silicon dust particles during silicon device processing.

EXPERIMENTAL METHOD

Gas phase silicon cluster ions are created by laser evaporation of a stationary bulk silicon target located just outside of a differentially pumped dual ion cell of a modified Nicolet FT/MS-1000 Fourier transform mass spectrometer (FTMS), Fig. 2 (Refs. 6,9). Direct laser evaporation produces both positively and negatively charged silicon clusters containing from 1-7 or 1-6 atoms, respectively. Additionally, electron impact ionization of SiD_4 is used to create the subsilane ions, SiD_{1-3}^{+}. The initial ion population is reduced to the cluster or subsilane ion of interest using double resonance techniques to select a single cluster size.

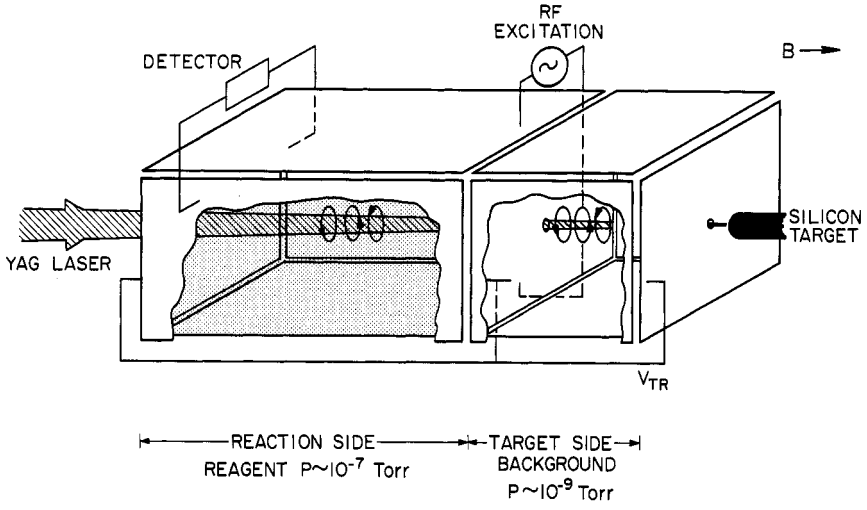

Fig. 2. FTMS dual ion cell depicting the silicon target for laser evaporation (532 nm, 300 MW/cm^2). The FTMS is operated in a solenoid magnetic field (B) of 2.96T and trapping potentials (V_{TR}) of ±1.0V.

Exothermic ion-molecule reactions of the silicon cluster ions are studied by trapping the ions in the presence of 1-10×10^{-7} Torr of a reagent gas. Bimolecular reaction rates and products are monitored by recording the mass spectra of the ions in the cell at a sequence of reaction times. Mass spectra are typically obtained with mass resolutions of at least 10,000 which permits straightforward separation of mass doublets such as $^{30}Si^{+}$ and $^{28}SiD^{+}$. Time dependencies of the normalized reactant and product ion intensities are analyzed to determine the rate associated with a given reaction. Exponential decays are pseudo-first-order since the reagent concentration is much greater than the ion concentration. All decays scale linearly with reagent pressure, with the exception of bimolecular attachment reactions which are second order in pressure. Fig. 3 shows, for example, the decay of Si_5^{-} in the reaction with NO_2 (Ref. 6). Although neutral products are not directly observed, they can often be deduced from thermodynamic information.

All of the products and rates are obtained under conditions which ensure that they will pertain to the exothermic reactions of ground state ion species which are thermally equilibrated with the cell temperature at 300K. For example, low electron energies and collisional relaxation are employed to produce a thermalized initial ion population. Absolute rate constants are calculated using the ion gauge pressure reading corrected for the differential pressure between the ion gauge and the ion cell as well as for the response factor of the ion gauge to various reagent gasses.

RESULTS AND DISCUSSION

Positively and negatively charged silicon clusters react exothermically with a variety of neutral reagents. Prototypical etching reactions are observed with a number of inorganic reagent molecules, including NO_2, XeF_2, ClF_3, and O_2. Prototypical deposition reactions are seen in reactions of silicon cluster cations with SiD_4. Such prototypical etching and deposition reactions are observed to occur sequentially to decrease or increase, respectively, the size of the silicon framework of the starting cluster.

Examples of the two distinct types of reactivity are described below. Then, the sequential cluster growth reactions with

SiD_4 are described for the starting ion, SiD_3^+. Last, the sequential clustering reactions are discussed as possible routes to the formation of silicon dust particles in silane plasmas.

Reactivity with NO_2: prototypical etching

NO_2 reacts exothermically with both positively and negatively charged silicon cluster ions (Ref. 6). As shown by Fig. 3, the predominant reaction is one where the silicon cluster ion is "etched" by NO_2, losing a silicon atom in the form of SiO; Eqs. 1-2.

$$Si_n^+ + NO_2 \rightarrow Si_{n-1}^+ + SiO + NO \quad (1)$$

$$Si_n^- + NO_2 \rightarrow Si_{n-1}^- + SiO + NO \quad (2)$$

Incorporation of oxygen in the clusters is a minor reaction, particularly for the larger clusters. Probabilities for these reactions as a function of cluster size are shown in Fig. 4 (Ref. 6). For the negatively charged clusters, charge transfer to NO_2 also occurs for Si_{1-4}^-. No electron transfer is seen for Si_{5-6}^-, a result of their large electron affinities of between 2.6 - 3.6 eV (Refs. 6,17).

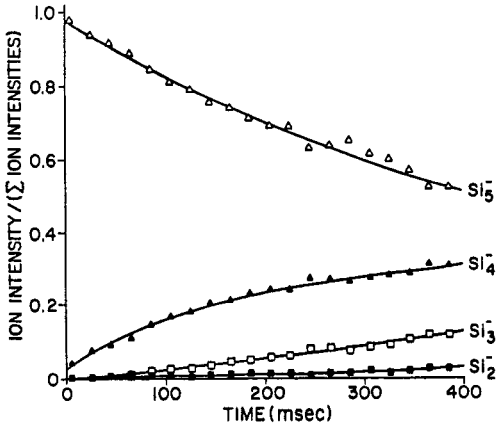

Fig. 3. Time evolution of the evolving ion populations in the reactions of Si_5^- with 9×10^{-8} Torr of NO_2. Their time dependences indicate that Si_4^- is a primary product, whereas Si_3^- and Si_2^- are higher order products.

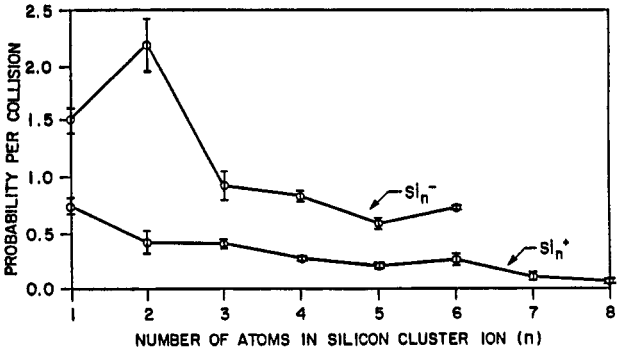

Fig. 4. Probability of silicon cluster reactions with NO_2 as a function of cluster size. The probability is calculated as the measured reaction rate divided by the ion-molecule reaction rate determined using the average dipole orientation theoretical model.

The similarity of the reactivity of cationic and anionic silicon clusters suggests that they react with NO_2 by a similar mechanism. The thermodynamics (Ref. 6) and reaction probabilities of these reactions indicate that the etching reaction occurs along a well-defined pathway involving one or more energetic barriers which increase with increasing cluster size. Finally, the reaction pathway prevents oxygenation of the cluster, despite the large strength of Si-O-Si bonds. Based on our data and similar reactions known for silicon-centered radicals (Ref. 18), we propose the mechanism illustrated for Si_4^+ in Fig. 5. Central to this mechanism is the coupling of a *radical* electron on a silicon atom in the clusters with the radical electron on NO_2. Undoubtedly this mechanism is oversimplified, however, it represents the simplest conceivable process which accounts for the observed reactions.

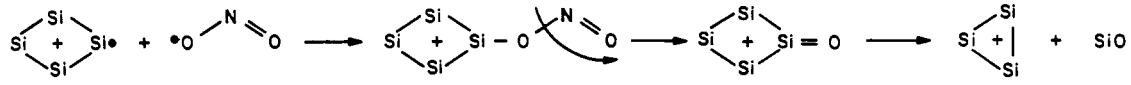

Fig. 5. Proposed reaction pathway for the reaction of Si_4^+ with NO_2 involving the interaction of a radical center on the cluster with the radical electron of NO_2.

The initial interaction probably occurs between the charged center on the silicon cluster and the oxygen of NO_2, followed by formation of a silicon-oxygen bond. Bonding between the radical electron on an oxygen atom in NO_2 and a radical electron on the silicon cluster is expected to be the lowest energy pathway. Energetically, formation of the $[Si_n–ONO]^+$ or $[Si_n–ONO]^-$ intermediate is highly favorable. Based on the energetics of Si-O bonds and the NO bond strengths of NO_2 versus NO_2R, we estimate that these intermediates lie at least 3eV below the reactants (Ref. 6). Thus, loss of NO, the weakest bound fragment, probably occurs almost simultaneously with Si-O bond formation. The resulting $[Si_nO]^+$ or $[Si_nO]^-$ intermediate further decomposes by loss of SiO. Extrusion of SiO appears to occurs while the oxygen is still bound as a terminal Si=O species, before the $[Si_nO]^{+/-}$ intermediate can rearrange to a more stable bridging Si-O-Si structure. This can be inferred because terminal Si=O centers are known to be highly unstable and lead to loss of SiO, whereas Si-O-Si bonds are among the strongest chemical bonds known. An analogous loss of SiO is known to occur when oxygenated silicon surfaces are reduced, such as during the processing of silica glasses.

Of course, standard etching processes for bulk silicon surfaces do not use NO_2. Therefore, we have also examined the reactions of silicon clusters with more typical etchant gasses such as XeF_2 and ClF_3. These reagents also remove silicon atoms from the silicon clusters exothermically at room temperature. The "etching" reactions, however, are not as simple as for NO_2 and usually two sequential reactions are required in order to remove one silicon atom. Further descriptions of these reactions can be found elsewhere (Ref. 7).

Reactivity with SiD_4: prototypical deposition

Positively charged silicon clusters react exothermically with SiD_4 to form larger deuterated silicon cluster ions (Refs. 10-12). The most common reaction is addition of a silicon atom to the cluster in the form of SiD_2,

$$Si_n^+ + SiD_4 \rightarrow Si_{n+1}D_2^+ + D_2 \tag{3}$$

As shown in Table 1, such prototypical deposition reactions are only observed for positively charged silicon clusters containing 1-3 and 5 atoms. Negatively charged silicon clusters do not react exothermically with silane to any appreciable extent during our experimental time scales.

The observed deposition reactions continue sequentially, forming larger deuterated silicon cluster ions by stepwise addition of a SiD_x moiety. For example, Si_3^+ is observed to add three silicon atoms during the time of our experiments,

$$Si_3^+ + SiD_4 \rightarrow Si_4^+ + 2D_2 \tag{4}$$

$$\rightarrow Si_4D_2^+ + D_2 \tag{5}$$

$$Si_4D_2^+ + SiD_4 \rightarrow Si_5D_4^+ + D_2 \tag{6}$$

$$Si_5D_4^+ + SiD_4 \rightarrow Si_6D_6^+ + D_2\ . \tag{7}$$

Note that the Si_4^+ produced in the initial reaction, Eq. 4, does not react further with SiD_4. This is consistent with the behavior of the Si_4^+ ion population produced initially by laser evaporation which also does not react with SiD_4. In addition, the growth sequence reaches a bottleneck at $Si_6D_6^+$ which either reacts very slowly with SiD_4 or not at all. As another illustration of sequential growth, Si^+ is observed to grow incrementally by three stepwise reactions,

$$Si^+ + SiD_4 \rightarrow Si_2D_2^+ + D_2 \tag{8}$$

$$Si_2D_2^+ + SiD_4 \rightarrow Si_3D_4^+ + D_2 \tag{9}$$

$$Si_3D_4^+ + SiD_4 \rightarrow Si_4D_6^+ + D_2\ . \tag{10}$$

Further growth of $Si_4D_6^+$ only occurs by inefficient bimolecular attachment,

$$Si_4D_6^+ + SiD_4 \rightarrow Si_5D_{10}^+ \tag{11}$$

Thus the sequential clustering reactions of Si^+ and Si_3^+ with SiD_4 are constrained to small cluster sizes. This constraint is seen for all of the reactive clusters, $Si_{1-3,5}^+$.

Electronic structure calculations have been started in order to characterize the mechanistic details of the silicon cluster reactions with silane. In the case of Si^+, extensive calculations have been performed on each of its sequential growth reactions (Ref. 12). Here it is found that each of the reactions proceed via an initial transition state involving insertion into one of the Si-D bonds of SiD_4. Loss of D_2 occurs from the resulting intermediate by a second elimination transition state. The insertion transition state requires a four-center transition state for $Si_2D_2^+$, $Si_3D_4^+$, and $Si_4D_6^+$. Elimination also involves a four center transition state. The calculated structure of these two transition states is shown below, Fig. 6, for the reaction of $Si_2D_2^+$ with SiD_4 (Ref. 12).

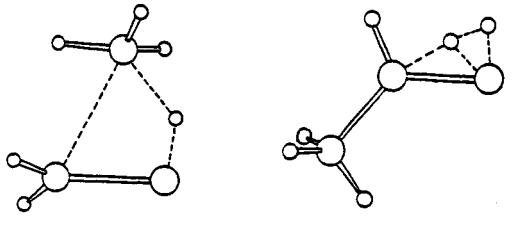

Fig. 6. Calculated structure of the Si-D bond insertion (left) and D_2 elimination (right) transition states during the reaction of $Si_2D_2^+$ with SiD_4. Both are four center transition states involving two adjacent silicon atoms.

No similar detailed calculations are available for the reactions of silicon clusters with silane. However, the smaller clusters also have unsaturated Si-Si bonds which can be expected to insert into Si-D bonds and eliminate D_2 in an analogous fashion. Insertion and elimination reactions of neutral silicon centers with silanes and hydrogen are quite well

known in silicon chemistry (Ref. 19). Here too, the potential energy surfaces have been theoretically investigated, but the essential transition states involve only a three center interaction (Ref. 20).

Three clusters, Si_4^+, Si_6^+ and Si_7^+, do not react exothermically with SiD_4 on the time scale of our experiments. The inertness of Si_4^+ appears to be related to its unusually stable structure, which makes reaction with SiD_4 slightly endothermic. Si_4^+ does react with a related reagent, CH_3SiH_3, by addition of either $SiCH_4$ or $SiCH_2$ to the cluster. The two largest silicon cluster cations that we have studied, Si_{6-7}^+, however, do not react either with SiD_4 or CH_3SiH_3. Thus, these larger clusters do not appear to have the necessary dangling bonds required for "deposition" type reactivity. The four center transition state mechanism involves an unsaturated silicon center adjacent to a divalent silicon atom on the cluster. Unlike the smaller clusters, the larger silicon clusters with six or more atoms have increased intramolecular silicon-silicon bonding with little or no divalent character. This suggests that Si_6^+, Si_7^+, *and all larger clusters* can not access a favorable transition state for activation of Si-D bonds.

The inertness of the larger silicon clusters in the prototypical deposition reactions with silane contrast to the deposition reactivity with NO_2 where reactivity persists for all cluster sizes. The proposed mechanisms provide a useful framework for understanding the fundamental difference between these two different types of reactivity. Silicon cluster deposition type reactivity requires adjacent unsaturated silicon centers and availability of two electron dangling bonds. Such reactive centers disappear as the cluster size increases and intramolecular bonding increases. Etching type reactivity involves one electron dangling bonds which persist despite the increase in silicon-silicon bonding for larger clusters.

Table 1. Sequential Clustering Reactions of Si_{1-7}^+ with SiD_4.[a]

Reaction	Product Fraction (%)	Rate Constant ($\times 10^{10}$)
$Si^+ + SiD_4 \rightarrow Si_2D_2^+ + D_2$	85 ± 4	8.1 ± 0.4
$Si_2^+ + SiD_4 \rightarrow Si_3D_2^+ + D_2$	100	2.5 ± 0.4
$Si_3^+ + SiD_4 \rightarrow Si_4^+ + 2D_2$	14 ± 2	4.8 ± 0.7
$\rightarrow Si_4D_2^+ + D_2$	86 ± 2	
$Si_4^+ + SiD_4 \rightarrow$ N. R.	100	≤0.006
$Si_5^+ + SiD_4 \rightarrow Si_6D_2^+ + D_2$	58 ± 5	0.8 ± 0.1
$\rightarrow Si_6D_3^+ + D$	41 ± 5	
$Si_6^+ + SiD_4 \rightarrow$ N. R.	100	≤0.001
$Si_7^+ + SiD_4 \rightarrow$ N. R.	100	≤0.005

[a]"N. R." indicates that no reaction products have been observed for a particular reacting ion. Reactions here are all exothermic with ground state ions at 300K. Neutral species are inferred from thermodynamics. Rate constants are given in units of cm^3 $molecule^{-1}$ sec^{-1}.

Table 2. Sequential Clustering Reactions of SiD_3^+ with SiD_4.[a]

Reaction[a]	Rate Constant[b] ($\times 10^{10}$)
$SiD_3^+ + SiD_4 \rightarrow Si_2D_5^+ + D_2$	0.6 ± 0.1
$\rightarrow Si_2D_7^+$	0.006 ± 0.002[d]
$Si_2D_5^+ + SiD_4 \rightarrow Si_3D_7^+ + D_2$	0.16 ± 0.05
$\rightarrow Si_3D_9^+$	0.12 ± 0.05
$Si_3D_7^+ + SiD_4 \rightarrow Si_4D_9^+ + D_2$	<0.0001
$\rightarrow Si_4D_{11}^+$	.0023 ± 0.0004

[a]Reactions are exothermic at room temperature. Neutral products have been inferred from thermodynamics. Rate constants are given in units of cm^3 $molecule^{-1}$ sec^{-1}.
[b]Rate constants are first order in SiD_4 pressure except for the association reactions, Eqs. 14-16, where they are second order in SiD_4 pressures. The reactions forming $Si_2D_7^+$, $Si_3D_9^+$, and $Si_4D_{11}^+$ were measured at $P(SiD_4) = 1.4 \times 10^{-6}$, 2.0×10^{-6}, and 5.6×10^{-6} Torr, respectively.

Cluster growth: sequential clustering reactions of SiD_3^+ with SiD_4

As described above, certain silicon clusters react stepwise with SiD_4 to form larger deuterated silicon clusters. SiD_3^+ is also observed to undergo sequential clusterings with SiD_4, Table 2 (Ref. 14). The mechanism of these reactions, however, is not the same as for Si^+ and the other reactive clusters. SiD_3^+ and the larger clusters that it forms, $Si_2D_5^+$ and $Si_3D_7^+$, are saturated in deuterium. The remaining electron is lost in forming the positive ion. Therefore, reaction of these species with SiD_4 must involve a mechanism distinct from that discussed above for Si^+.

Incremental growth of SiD_3^+ occurs by addition of SiD_2 accompanied by loss of D_2,

$$SiD_3^+ + SiD_4 \rightarrow Si_2D_5^+ + D_2 \quad (12)$$

$$Si_2D_5^+ + SiD_4 \rightarrow Si_3D_7^+ + D_2 \quad (13)$$

This SiD_2 addition process stops with at $Si_3D_7^+$; a third reaction to form $Si_4D_9^+$ does not appear to occur. Formation and stabilization of an association complex with SiD_4 is also observed,

$$SiD_3^+ + SiD_4 \xrightarrow{M} Si_2D_7^+ \quad (14)$$

$$Si_2D_5^+ + SiD_4 \xrightarrow{M} Si_3D_9^+ \quad (15)$$

$$Si_3D_7^+ + SiD_4 \xrightarrow{M} Si_4D_{11}^+ . \quad (16)$$

On the time scale of our experiments, the sequential growth reactions do not proceed beyond the formation of the four-silicon species. No other exothermic products are observed in these reactions with silane. The same products are seen when reactions are performed with the perprotiated species, SiH_3^+ and SiH_4.

The mechanisms and energetics of the microscopic pathways for the sequential clustering reactions of SiD_3^+ with SiD_4 have been determined by Raghavachari using *ab initio* electronic structure calculations (Ref. 15). All three observed steps in the clustering sequence are found to involve similar microscopic pathways. Overall, these reactions proceed by formation of a strongly bound deuterium bridged intermediate complex. This intermediate reaction complex can fall apart to reactants or be collisionally stabilized to give the observed association products, Eqs. 14-16. Elimination of D_2 occurs via a near thermoneutral transition state which leads to the SiD_2 addition products, Eqs. 12-13. In the second reaction, the linear $Si_3D_7^+$ product is calculated to rearrange to a more stable cyclic deuterium bridged structure, *c*-SiD_2–SiD_2–SiD_2–D^+. It is the energetic favorability of this cyclic $Si_3D_7^+$ structure which halts the next addition of SiD_2.

Qualitatively, the reaction pathways calculated by Raghavachari agree well with the experimentally observed reaction sequence and explain why exothermic cluster growth stops. Given the existence of alternative mechanisms, it is important to have experimental evidence to quantitatively verify these calculated reaction pathways. Using the statistical phase space theory (PST) of Chesnavich and Bowers, our experimental reactions rates afford a means of quantitatively testing the energies of a number of the calculated structures (Ref. 21). In the PST model calculations, the probabilities of formation of the bimolecular addition products, Eqs. 14-16, are extremely sensitive to the binding energy of the deuterium bridged reaction intermediates. Similarly, probabilities of SiD_2 addition, Eqs. 12-13, are extremely sensitive to the energetics of the elimination transition states. Thus, the energetics derived from our experimental reaction probabilities provide a quantitative test of the accuracy of several key points on the potential surface calculated by Raghavachari.

A detailed description of our PST model calculations is outside the scope of this brief review. The overall approach involves calculating the forward and backward rates in the competing kinetic processes during the reaction,

$$SiD_3^+ + SiD_4 \underset{k_D}{\overset{k_C}{\rightleftharpoons}} [(SiD_3)\cdots D\cdots(SiD_3)^+]^\dagger \xrightarrow{k_E} Si_2D_5^+ + D_2 \quad (17)$$

$$\xrightarrow{k_S[M]} Si_2D_7^+ \quad (18)$$

$$\xrightarrow{k_R} Si_2D_7^+ \quad (19)$$

In Eqs. 17-19, K_C and K_D are the forward and back reaction rates for the formation of the deuterium bridged intermediate complex, respectively. K_E is the rate of formation of the SiD_2 addition product. The observed association product, $Si_2D_7^+$, is formed from the activated $[Si_2D_7^+]^\dagger$ via collisional stabilization by a third body, M, with a rate K_S, or via radiative stabilization at a rate, K_R. Extensive details in the methods of evaluating these quantities are given in Refs. 10,14. In all cases, agreement in transition state and intermediate complex energies is within 0.13 eV, less than 3 kcal/mole, which is remarkably good considering the simplifying assumptions used in the PST calculations and the degree of accuracy of the *ab initio* calculations.

The experimental tests of the *ab initio* calculations of the mechanisms of the SiD_3^+ clustering reactions with SiD_4 are crucial verifications that Raghavachari has succeeded in describing these reactions at the microscopic level. Similar good quantitative agreement between experiment and electronic structure calculations was also obtained for the sequential clustering reactions of Si^+ with SiD_4 (Refs. 10,12). The implications of this are tremendous, particular for neutral-neutral clustering reactions involving subsilanes. In these neutral systems, quantitative experiments have not been made, and are inherently so difficult that they are not likely to be carried out in the near future. Good theoretical calculations could provide the data needed to understand these reactions.

SiD_3^+ sequential clustering reactions with SiD_4: implications for formation of Si:H particulates in silane plasmas

Formation of hydrogenated silicon dust plagues the growth of high quality silicon films from silane vapors and plasmas (Refs. 22-23). The essential mechanism governing the growth of these particles continues to elude experimental and kinetic modeling investigations (Ref. 24). Some relevant information has, however, been uncovered. In silane plasmas, positively charged species appear to be responsible for particle formation (Refs. 24-25). There is a noticeable delay between the start of the discharge and the appearance of this dust. This indicates that some time is required for them to grow in the gas phase. And, their appearance is sensitive in a complex fashion to the temperature, pressure, and rf power of the discharge.

Any investigation of the microscopic pathways which might lead to dust formation should start with SiH_3^+ and its sequential clustering reactions with SiH_4. The reason for this is simple: *SiH_3^+ is the most abundant initial SiH_x^+ ion in silane plasmas* (Ref. 24). A recent calculation shows that SiH_3^+ is ten times more abundant in SiH_4 plasmas than any of the other three subsilane cations, SiH_{0-2}^+ (Ref. 26).

But is SiH_3^+ the actual precursor ion which leads to formation of hydrogenated silicon dust by sequential reactions with SiH_4? Although we can not be sure, our results suggest not. The primary reasons are that the sequential clustering reactions for SiH_3^+ and its "progeny" with SiH_4 are quite slow and lead quickly to bottleneck species which are highly coordinated in hydrogen. SiH_3^+ clustering reactions with SiH_4 are at least an order of magnitude slower than comparable reactions for clustering sequences of SiH_{0-2}^+ (Refs. 10,16). Kinetically, this leads to a cumulative effect where all of the other SiH_x^+ initial ions quickly react away to form larger $Si_xH_y^+$ species, leaving SiH_3^+ behind. All of the bimolecular association products, $Si_2H_7^+$, $Si_3H_9^+$, $Si_4H_{11}^+$, etc. are also bottleneck species. Since all of the silicon atoms in these species are saturated, further interactions of these structures with silane are expected to be quite weak, governed by small long range ion-induced dipole forces (Ref. 15). The other bottleneck structure is $Si_3H_7^+$. Due to its stability, the $Si_3H_7^+$ cyclic structure cannot access the H_2 loss pathway in a reaction with SiH_4 because the H_2 elimination transition state lies energetically above the reactant energy. The subsequent $Si_4H_9^+$ and $Si_5H_{11}^+$ ions, were they to be formed, would also be expected to be bottleneck species with stable cyclic structures similar to that of $Si_3H_7^+$ (Ref. 15).

Different temperature and pressure conditions in silane plasmas might be expected to overcome the kinetic and thermodynamic bottlenecks preventing rapid clustering of SiH_3^+ with SiH_4. Commercial plasma deposition of amorphous silicon films is performed with typical operating temperatures ranging from 300 - 600K and gas pressures ranging from 10 - 1000 mTorr with 1-50% silane. Therefore, it is important to study the sequential clustering reactions of SiH_3^+ with SiH_4 under "real" conditions. This is not a problem! Since we know the important microscopic details of the potential surfaces for the clustering reactions from Raghavachari's calculations, we can easily compute all of the reaction probabilities for SiH_2 addition and SiH_4 association at elevated temperatures and pressures, Figs. 7-8. Increasing the gas temperature does not increase the SiH_2 addition probabilities above about 2%, and drastically slows down the association reactions, Fig. 7. Increasing the gas pressure favors formation of the association products, Fig. 8. For example, at 600K and 100 mTorr of SiH_4, the association products, $Si_2H_7^+$, $Si_3H_9^+$, $Si_4H_{11}^+$, and $Si_5H_{13}^+$ are favored at each clustering step during the growth sequence. Thus, the net effect of the increased pressure and temperature conditions in plasma reactors does not appear to overcome the bottlenecks to infinite growth by SiH_2 addition.

In summary, while SiH_3^+ is the most abundant subsilane ion in SiH_4 plasmas, its reactions with SiH_4 do not appear to explain the formation of hydrogenated silicon dust. SiH_3^+ simply reacts too slowly and forms too many "dead-end" structures. We have also examined clustering reactions of the other subsilane cations, SiH_{0-2}^+ and the bare silicon cluster ions, Si_{2-7}^+ (Ref. 10-12,16). In all cases, we find that sequential growth stops at cluster sizes well below the critical nucleus size required for rapid spontaneous growth. Two general reasons govern termination of the cluster sequence. In the cases of Si^+ and SiH_3^+ described above, clustering stops when hydrogen saturates the reactive site on the cluster. Alternatively, especially for the bare clusters, clustering leads to more compact structures with increased intramolecular silicon-silicon bonding and loss of the reactive centers.

Of course, this hydrogenated dust must form! Our results suggest that attention must be paid to alternative formation mechanisms. One possible route is via clustering of negatively charged ions with silane as reported in Ref. 27. Such a route would be highly inefficient as these negative ion clustering reactions are extremely slow, ≤0.05% of the ion-molecule collision rate. Additionally, neutral - neutral clustering or ionic sputtering of particulates from the electrode surfaces may lead to particle formation. Little data is available on these possible mechanisms. Clearly, further investigations are warranted in order to engineer methods for particle control or prevention.

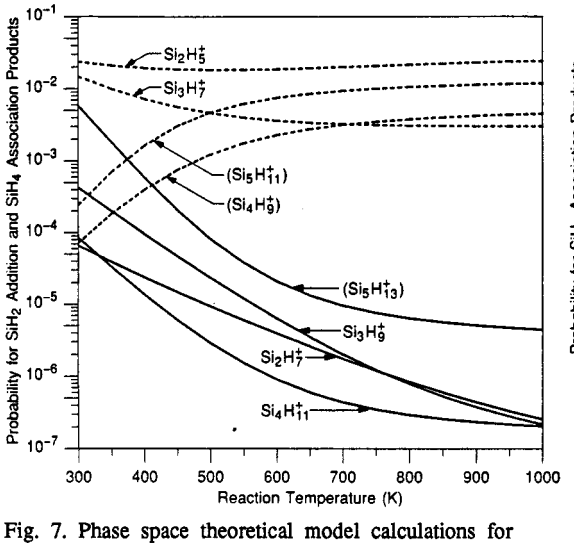

Fig. 7. Phase space theoretical model calculations for the formation probabilities of the SiH_2 addition and SiH_4 association products as a function of temperature.

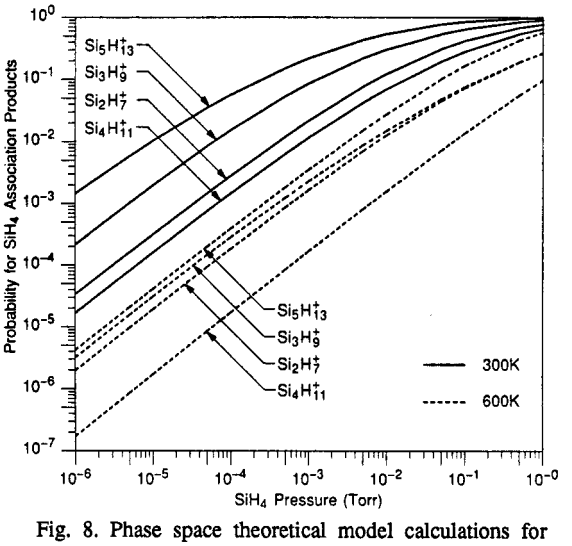

Fig. 8. Phase space theoretical model calculations for the formation probabilities of the SiH_4 association products as a function of SiH_4 pressure at 300K and 600K.

CONCLUSIONS

Silicon clusters are unusual, highly reactive forms of silicon matter. Despite the many differences between clusters and bulk surfaces, these small clusters may well resemble the highly reactive silicon species at silicon defects and active surfaces produced by ion bombardment, pyrolysis, or photochemical activation.

These clusters exhibit exothermic prototypical deposition and etching reactions with organic and inorganic reagents at room temperature. Different types of dangling bonds on the silicon centers appear to be involved in etching versus deposition type reactivity.

Experimental measurements and electronic structure calculations, in concert, give insights into unforeseen mechanisms for silicon centered reactions with silane. These mechanisms are responsible for stepwise cluster growth in these reactions and also for termination of this growth at small cluster sizes. Limitations to growth occur because of deuterium saturation of the reactive center, formation of certain highly stable structures, or formation of larger, more compact silicon clusters. Our findings suggest that the origin of the deleterious hydrogenated silicon dust in silane plasmas cannot be explained by infinite sequences of growth via reactions of small cationic silicon clusters or subsilane cations with silane.

REFERENCES

1. K. Raghavachari and V. Logovinsky, Phys. Rev. Lett. 55 , 2853-2856 (1985).
2. K. Raghavachari, J. Chem. Phys. 84 , 5672-5686 (1986).
3. G. Pacchioni and J. Koutecky, J. Chem. Phys. 84 , 3301-3310 (1986).
4. K. Balasubramanian, Chem. Phys. Lett. 135 , 283-287 (1987).
5. K. Raghavachari, J. Chem. Phys. , submitted: "Theoretical Study of Small Silicon Cluster Ions of Si_2 - Si_6."
6. M. L. Mandich, V. E. Bondybey, and W. D. Reents, Jr. J. Chem. Phys. 86 , 4245-4257 (1987).
7. W. D. Reents, Jr., A. M. Mujsce, V. E. Bondybey, and M. L. Mandich, J. Chem. Phys. 86 , 5568-5577 (1987).
8. W. R. Creasy, A. O'Keefe, and J. R. McDonald, J. Phys. Chem. 91 , 2848-2855 (1987).
9. M. L. Mandich, W. D. Reents, Jr. and V. E. Bondybey, J. Phys. Chem. 90 , 2315-2319 (1986).
10. M. L. Mandich, W. D. Reents, Jr., and M. F. Jarrold, J. Chem. Phys. 88 , 1703-1718 (1988).
11. M. L. Mandich and W. D. Reents, Jr. J. Chem. Phys. 90 , 3121-3135 (1989).
12. K. Raghavachari, J. Chem. Phys. 88 , 1688-1702 (1988).
13. W. D. Reents, Jr. and M. L. Mandich, J. Phys. Chem. 92 , 2908-2912 (1988).
14. M. L. Mandich, W. D. Reents, Jr., and K. D. Kolenbrander, submitted to J. Chem. Phys.
15. K. Raghavachari, submitted to J. Chem. Phys.
16. M. L. Mandich and W. D. Reents, unpublished results.
17. W. D. Reents, Jr., M. L. Mandich, and V. E. Bondybey, Chem. Phys. Letts. 131 1-7 (1986).
18. J. W. Wilt in Reactive Intermediates, Vol. 3, R. A. Abramovitch, ed., 113-197, Plenum Press, New York (1983).
19. See, for example, P. P. Gaspar in Reactive Intermediates, Vol. 3, M. Jones, Jr. and R. A. Moss, eds., 333-427, Wiley, New York, (1985); Y. Tang in Reactive Intermediates, Vol. 2, R. A. Abramovitch, ed., 297-366, Plenum Press, New York, (1982).
20. K. K. Baldridge, J. A. Boatz, S. Koseki, and M. S. Gordon, Ann. Rev. Phys. Chem. 38 , 211-252 (1987).
21. W. J. Chesnavich and M. T. Bowers, Prog. in React. Kinet. 11 , 137-268 (1982).
22. F. C. Eversteijn, Philips Res. Reports 26 , 134-144 (1971).
23. S. M. Sze, ed., VLSI Technology , 51-91, McGraw-Hill, New York (1983).
24. See M. J. Kushner, J. Appl. Phys. 63 , 2532-2551 (1988), and references therein.
25. H. A. Weakliem, R. D. Estes, and P. A. Longeway, J. Vac. Sci. Technol. A5 , 29-36 (1987).
26. H. Chatham and A. Gallagher, J. Appl. Phys. 58 , 159-169 (1985).
27. J. Perrin, A. Lloret, G. De Rosny, and J. P. M. Schmitt, Int. J. Mass Spectrom. Ion Proc. 57 , 249-281 (1984).